

CHANDRA OBSERVATION OF THE MERGING CLUSTER A168: A LATE STAGE IN THE EVOLUTION OF A COLD FRONT

ERIC J. HALLMAN¹ AND MAXIM MARKEVITCH^{2,3}

Draft version September 23, 2018

ABSTRACT

We present *Chandra* observations of the cool cluster A168, for which previous X-ray imaging and optical studies indicated a merger of two subclusters nearly in the plane of the sky. We derive a temperature map for A168, which shows that the merger has proceeded beyond the core passage and is near subcluster turnaround. It also reveals an unusual feature — the gas core of one of the subclusters forms a tongue-like structure extending ahead (in the direction of motion) of the subcluster center. The coolest cluster gas is found in a crescent-shaped region at the tip of this tongue, and forms a cold front in pressure equilibrium with the external gas. In contrast with this feature’s forward location, previously observed merger cold fronts (e.g., A3667, 1E0657–56) lagged behind their host subclusters, as expected in the presence of ram pressure. We propose that A168 illustrates a much later stage in the evolution of a cold front, when its host subcluster approaches the apocenter of the merger orbit where the ram pressure on its gas drops sharply. As a result, a large chunk of the subcluster gas “slingshots” past the dark matter center, becomes unbound from the subcluster and expands adiabatically, as seen in some recent hydrodynamic simulations.

Subject headings: Galaxies: clusters: individual (A168) — intergalactic medium — X-rays: galaxies

1. INTRODUCTION

Galaxy clusters form via infall and merger of larger subunits. Such mergers generate a wealth of transient hydrodynamic phenomena in the intracluster gas that can be studied in X-rays, most notably shocks (e.g., Schindler & Müller 1993; Burns 1998; Ricker & Sarazin 2001). In addition, typical clusters have dense gas cores that appear to be able to survive a merger and form the prominent contact discontinuities, or “cold fronts”, revealed in *Chandra* high-resolution X-ray images of many merging and relaxed clusters (e.g., Markevitch et al. 2000; Vikhlinin, Markevitch & Murray 2001b; Markevitch, Vikhlinin, & Mazzotta 2001; Kempner, Sarazin, & Ricker 2002). Cold fronts are seen as sharp edges in the cluster X-ray images and temperature maps. The brighter side of the jump has a lower gas temperature than the faint side by a ratio similar to the density jump, indicating rough pressure balance across the front. This distinguishes cold fronts from the less frequently observed bow shock discontinuities in which the hotter side is also denser. Cold fronts are interpreted as a boundary of a dense subcluster core moving through a hotter ambient medium (Markevitch et al. 2000), though the term is often used to refer to the entire cold region. This phenomenon provides novel tools to study the cluster physics. For example, cold fronts are very sharp, with a width smaller than the electron Coulomb mean free path, which places severe upper limits on electron diffusion and thermal conduction across the front (Vikhlinin et al. 2001b; see also Ettori & Fabian 2000). A cold front in A3667 also indicates a parallel magnetic field is necessary to stabilize it against the onset of hydrodynamic instabilities (Vikhlinin et al. 2001a). Merger cold fronts have been reproduced in recent hydrodynamic simulations (e.g., Bialek, Evrard, & Mohr 2002; Nagai & Kravtsov 2003; Mathis et al. 2003), although

with limited spatial resolution.

This paper analyzes *Chandra* observations of A168 ($z = 0.045$). Earlier X-ray imaging of A168 with *Einstein* IPC revealed irregular structure indicative of a merger (Ulmer et al. 1992; Jones & Forman 1999). The ends of its extended X-ray structure coincide with two galaxy subclusters, the northern of which is dominated by a cD galaxy UGC 00797 and has few other members, while the rich southern subcluster has no dominant galaxy (Fig. 1a). More evidence of a merger is provided by a recent detailed optical study which shows that the redshift distributions of the two subclusters differ significantly (Yang et al. 2004). This interesting merger, apparently occurring near the plane of the sky, is the subject of this *Chandra* study. We use $H_0 = 70 \text{ km s}^{-1} \text{ Mpc}^{-1}$ and quote 90% confidence intervals throughout the paper.

2. DATA ANALYSIS

Two ACIS-I observations of A168 were done in 2002 January and November for 40 ks and 37 ks, respectively. The first pointing covered the northern region of the cluster, including the cD galaxy, and the second covered the southern X-ray elongation and overlapped with the first pointing. Our analysis procedure largely follows Markevitch & Vikhlinin (2001). The background was modeled using blank-sky files from the *Chandra* calibration database. A correction for the low-energy absorption caused by the ACIS contamination buildup (Plucinsky et al. 2003) was included in the ARFs. Point sources were masked out. The two offset pointings were co-added; the resulting combined ACIS image is overlaid on the DSS plate in Fig. 1a.

To study the global properties of the cluster, we extracted a 0.8–6 keV spectrum from a $r = 10'$ circle around the surface brightness centroid ($\alpha = 01:15:01$, $\delta = +00:20:26$) Using the Galactic absorption column $N_H = 3.48 \times 10^{20} \text{ cm}^{-2}$, we obtained $T_e = 2.8 \pm 0.1 \text{ keV}$, and a chemical abundance of 0.30 ± 0.05 relative to solar. This temperature is in good agreement with the earlier *Einstein* MPC measurement of $2.6^{+1.1}_{-0.6} \text{ keV}$ (David et al. 1993). However, as is seen below, the cluster is highly non-isothermal.

¹ Department of Astronomy, University of Minnesota, 116 Church St. SE, Minneapolis, MN 55455, hallman@astro.umn.edu

² Harvard-Smithsonian Center for Astrophysics, 60 Garden Street, Cambridge, MA 02138, maxim@head.cfa.harvard.edu

³ Space Research Institute, Profsoyuznaya 84/32, Moscow 117997, Russia

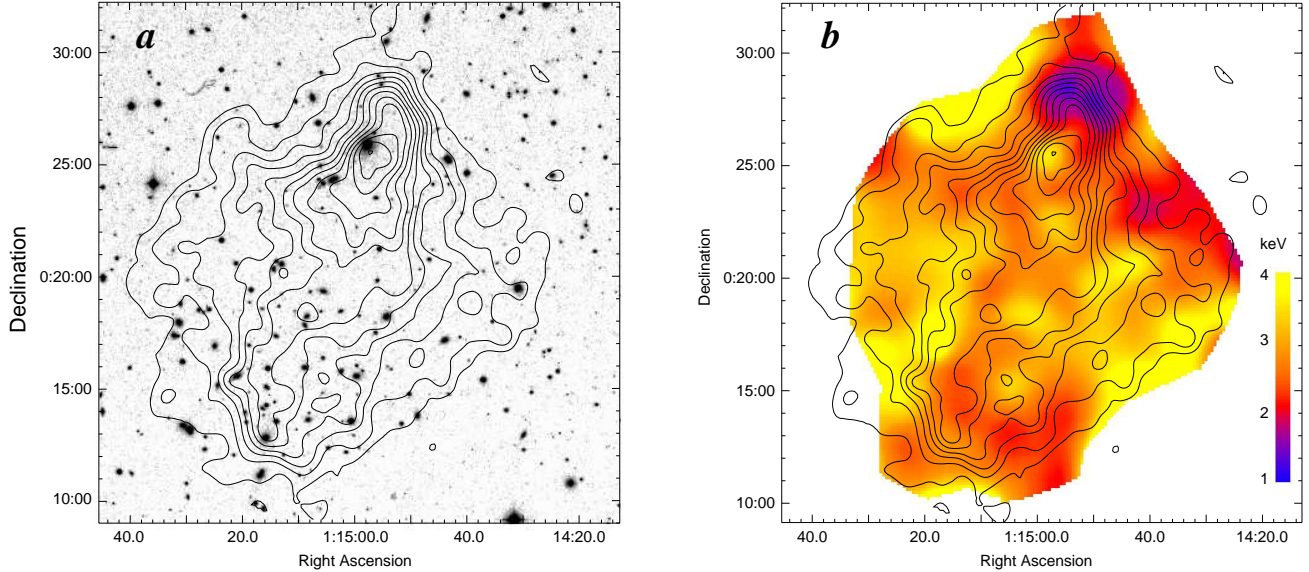


FIG. 1.— (a) Contours of 0.8–6.0 keV *Chandra* X-ray brightness (linear spacing; image smoothed by $\sigma = 24''$), overlaid on Palomar Digitized Sky Survey optical image of A168 field. (b) Projected temperature map (colors) overlaid with the image contours.

2.1. Temperature Map

We derived a projected temperature map by creating cluster images in 5 energy bands, 0.8–1.3–2–3–4–6 keV. These images were each adaptively smoothed by a Gaussian in the $\sigma = 20'' - 60''$ interval using an identical smoothing pattern. The flux values for each energy at each image pixel were fit by a MEKAL model with absorption set to the Galactic value and the chemical abundance set to the overall cluster value. The resulting map is shown in Fig. 1b, overlaid on the brightness contours. To check the significance of the temperature variations, and to look for abundance variations, we also extracted spectra from 12 regions of the image (Fig. 2) and performed the usual spectral fitting with either fixed or free abundances. No significant abundance variations are detected. Figure 2 shows the fits with fixed abundances; there is good agreement with the smooth temperature map.

The most striking feature in the temperature map and the X-ray image is the cool crescent-shaped region in the north. It does not coincide with the gas density peak approximately at the position of the cD galaxy, which would make it similar to many cooling flow clusters. Rather, it lies at the tip of the prominent tongue-like X-ray brightness feature extending 200 kpc north of the cD and ending with an apparent cold front. We will discuss this “northern front” in more detail below (§4).

Other interesting features in the temperature map include a cool region at the southern subcluster (region 9), a cool arm-like eastward X-ray extension (region 2), a symmetric cool feature less prominent in the X-ray image (region 10), and hotter areas on either side of the central brightness ridge (regions 3, 12 and part of 11). An important thing to note is that the temperature map *does not* show a characteristic hot region between the merging subclusters, such as we would expect if they were approaching each other at present (e.g., Ricker & Sarazin 2001; Belsole et al. 2003).

3. DYNAMICAL STATE OF A168

In a recent study of the A168 member redshifts, Yang et al. (2004) show that the galaxies near the northern X-ray peak

and the southern X-ray elongation separate into statistically distinct groups. They conclude that the northern and south-

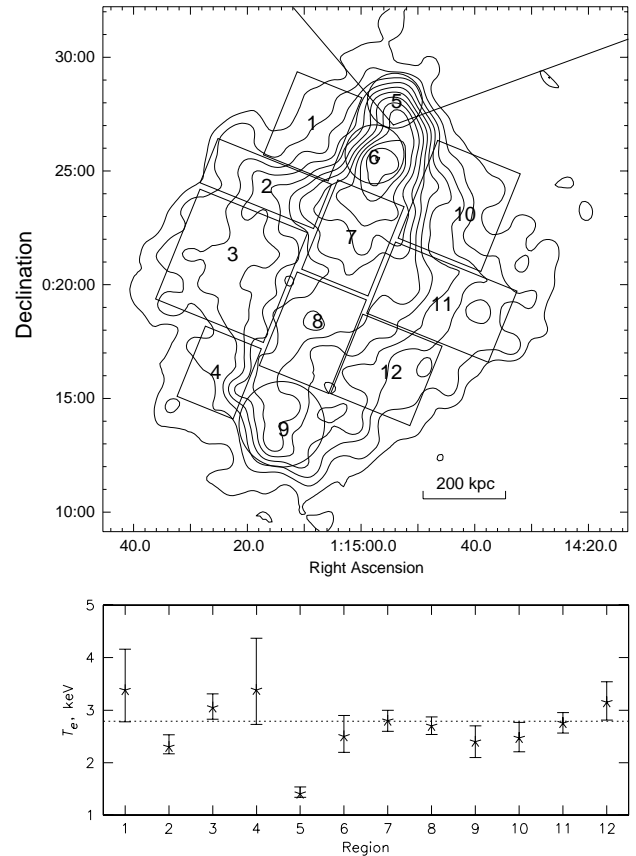


FIG. 2.— X-ray brightness contours overlaid with numbered spectral extraction regions. Underneath is plot of fitted temperature from spectra extracted from these regions. Dotted line is global cluster temperature fit. The two angled lines originating in region 5 are the sector border for the annular regions used for radial profiles.

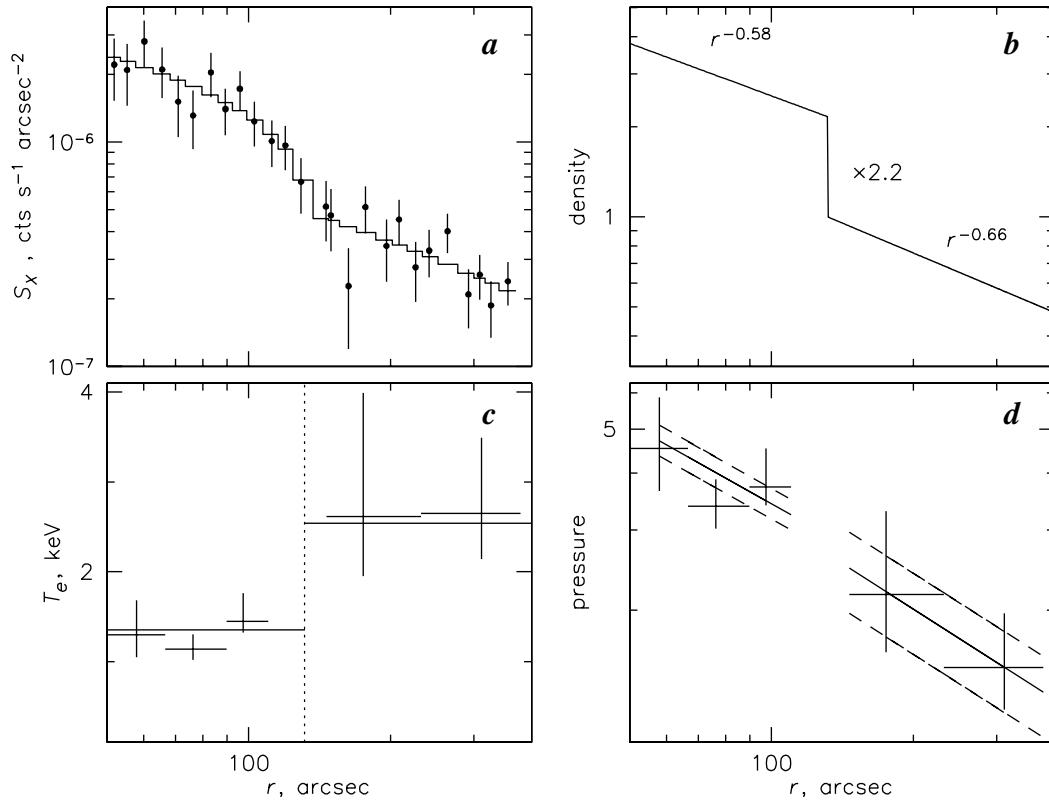


FIG. 3.— (a) 0.8–3.0 keV X-ray brightness profile across the northern front. Regions extracted for this profile use concentric annular sectors cut at the lines indicated in Fig. 2. Solid line is the brightness profile resulting from the projected best-fit spherical density model shown in (b). Density is in arbitrary units. (c) Temperature profile across the same front. Solid lines are the combined single temperature fits for all interior and all exterior regions, respectively. Vertical line indicates location of best-fit density jump. (d) Pressure profile generated from multiplication of the density model with the fitted spectral temperatures at each point. Solid lines indicate the pressure from the combined temperature fits inside and outside the jump, dashed lines are the errors for those. Units are arbitrary.

ern galaxy subgroups are on a collision course roughly in the plane of the sky. However, since the line of sight orientation of the subclusters is unknown, the determination of the direction of their relative motion from the redshift data alone is ambiguous, so the Yang et al. scenario for A168 is not unique.

The new X-ray data suggest a more likely scenario for the merger stage and geometry. The presence of the “northern front” indicates a motion of the northern subcluster in the northern direction (i.e., away from the other subcluster), either at present or very recently. An interpretation which better fits this observation, as well as the lack of shock-heated gas between the two X-ray peaks in our temperature map, is that the A168 subclusters have already passed one another at least once. Simulations, e.g., by Ricker & Sarazin (2001) and Mathis et al. (2003), support this interpretation. Immediately after one pass of subclusters, they predict an elongated appearance of the X-ray surface brightness and a ridge of cooler gas between the subcluster centers. In addition, Mathis et al. (2003) predict the qualitative features of the northern front very well; this is further discussed in §4.

In this late merger scenario, the marginally cooler southern subcluster (region 9 in Fig. 2) is an analog to the northern front, although not quite as prominent. The morphology of the temperature structure is qualitatively similar, in that the cold gas is displaced toward the tip of the X-ray elongation. The slightly hotter gas on the two sides of the cluster axis (regions 3 and 12) could be what remains of the shock-heated gas between the colliding subclusters that has had time to expand adiabatically as those subclusters have moved apart. The cool

eastern arm in region 2 may have analogs in A3667, where a similar feature was interpreted as a large-scale eddy created by Kelvin-Helmholtz instability (Mazzotta et al. 2002), and in simulations by Ricker & Sarazin.

4. THE NORTHERN FRONT

To study the pressure across the northern brightness edge, we extract a surface brightness and temperature profile from concentric elliptical annular regions (with the ellipse selected to follow the brightness edge) inside and outside the edge, confined to the sector between the two lines on Fig. 2. The 0.8–3.0 keV surface brightness in this sector is plotted in Fig. 3a. The solid line is a projection of the best-fit spherically symmetric (in the interesting region of space) density model that consists of two power-law radial profiles and an abrupt jump at a certain radius (Fig. 3b), all of which were free parameters. To compare the model to the brightness profile, we projected it and took into account the different emissivity due to the accompanying temperature change (see below). The best-fit density jump is a factor of $2.2^{+0.6}_{-0.4}$. The brightness jump is not as sharp as in some other clusters, with a transition region of roughly $30''$ or 27 kpc, a factor of a few wider than the upper limit on the width of the unresolved front in A3667 (Vikhlinin et al. 2001b). A possible explanation is a small nonzero angle of the subcluster velocity from the sky plane (e.g., Mazzotta et al. 2001).

A temperature profile across the edge is derived in wider annular regions in order to include sufficient counts. Since the edge is not particularly sharp, the inner and outer spectral re-

regions are separated by a $30''$ gap to avoid contamination of the outer regions by contribution from the brighter inner region. We performed an approximate deprojection of the contribution of the outer, hotter spherical regions to the inner spectra, using the density model fitted above. This resulted in a small temperature correction for the bins nearest to the edge. Figure 3c shows the resulting temperature profile. Also shown are a simultaneous fit for the spectral regions inside the edge, $T = 1.35 \pm 0.1$ keV, and for the outer regions, $T = 2.5^{+0.7}_{-0.4}$ keV. The individual bins are consistent with these averages on both sides of the jump. The ratio of these temperatures is $1.9^{+0.5}_{-0.3}$, the reverse of the density jump obtained above, which clearly identifies this feature as a cold front.

The temperatures and the density model provide a pressure profile across the front (Fig. 3d), which shows that thermal pressure is continuous within the errors. This indicates that the present velocity of the cool gas relative to the ambient gas is consistent with zero, with a 90% upper limit on the Mach number of $M < 0.7$ assuming a stationary flow (e.g., Vikhlinin et al. 2001a).

What makes the cold front in A168 unusual is that the gas is apparently not driven by, or lagging behind, the associated galaxy subcluster (Fig. 1a). This is in contrast to 1E0657–56 (Markevitch et al. 2002; Clowe et al. 2004) and A3667 (Vikhlinin & Markevitch 2002), the two cold fronts where the subcluster mass centroid could be located. The gas is expected to lag because, unlike dark matter, it is affected by the ram pressure of the ambient gas. Instead, the cool gas in A168 lies ahead of the cD galaxy that should be the center of the local gravitational potential.

The development of fronts like the one in A168 is predicted by simulations (most clearly those by Mathis et al. 2003) when a cool dense subcluster emerges from the collision site and is near its apocenter, but no clear physical explanation for such detachment was proposed. The simple explanation which we propose is one in which the ram pressure from the motion of the subcluster through the ambient medium initially pushes the gas backwards from the dark matter core centered on the cD galaxy, and it trails the dark matter as in other clusters. However, once the subcluster approaches the apocenter of its orbit, the ram pressure drops sharply due to the combination of reduced ambient gas density and lower subcluster velocity. At this point, the gas which was trailing the dark matter core “slingshots” past it (driven in part by the gas internal pressure and in part by the subcluster’s gravity) into the still lower density medium, while the underlying dark matter core turns around. The leading part of the gas core becomes unbound from the subcluster, expands, cools adiabatically and

forms the cold tip we observe in A168.

Heinz et al. (2003) predicted that the motion of a subcluster through a cluster medium should generate gas flows inside the subcluster which transport gas to its front edge, which alone should produce a crescent-shaped cool region near the front, just as observed in A3667 (Heinz et al.) and in our cluster. A combination of this process and the ram pressure “slingshot” proposed above fully explains the structure and location of the northern front in A168.

The A168 front resembles a cool-tipped gas tongue in A754, which was proposed to be the result of the gas “sloshing” out of a subcluster at an advanced merger stage (Markevitch et al. 2003). Unlike the messy A754, A168 is simple and shows this process more clearly.

An interesting implication of our A168 observation is that it shows how a large chunk of the cool subcluster gas unbinds from the subcluster and deposits itself into the ambient gas. Since it is in pressure equilibrium and has zero velocity relative to the ambient gas, it will persist there for a long time as a distinct region (e.g., Mathis et al. 2003). This shows that a merger is inefficient in mixing the different gas phases.

5. SUMMARY

We have analyzed *Chandra* observations of a merging cluster A168. The cluster brightness and projected temperature distribution suggest that the two subcluster cores have passed one another and are in the process of turning around. The coolest cluster gas is found at the tip of an interesting tongue-like structure, which extends ahead of the northern subcluster (i.e., away from the merger center) and ends with a cold front. This cold front differs from those observed earlier (e.g., in A3667 and 1E0657–56) which lag behind their host subclusters due to the ram pressure effects. A168 presents the first example of a cold front at a late stage of its evolution, when the subcluster reaches its apocenter, the ram pressure of the ambient gas sharply decreases and the leading part of the subcluster gas core “slingshots” ahead of its host dark matter concentration, expanding adiabatically and forming an offset cool region. According to simulations (Mathis et al. 2003), this cool gas will remain there as a distinct region as the dark matter subcluster falls back.

We thank Alexey Vikhlinin for his spectral analysis software and Bill Forman and Tom Jones for valuable comments. Support was provided by NASA contract NAS8-39073, *Chandra* grant GO2-3165X, the NSF grant AST03-07600, and the Minnesota Supercomputing Institute.

REFERENCES

- Belsole, E., Pratt, G. W., Sauvageot, J.-L., & Bourdin, H. 2003, A&A, in press (astro-ph/0311556)
- Bialek, J. J., Evrard, A. E., & Mohr, J. J. 2002, ApJ, 578, L9
- Burns, J. O. 1998, Science, 280, 400
- Clowe, D., Gonzalez, A., & Markevitch, M. 2004, ApJ, 604, 596
- David, L. P., Slyz, A., Jones, C., Forman, W. R., Vrtilek, S. D., Arnaud, K. A., 1993, ApJ, 412, 479
- Ettori, S., & Fabian, A. 2000, MNRAS, 317, 57L
- Heinz, S., Churazov, E., Forman, W., Jones, C., Briel, U. G., 2003, MNRAS, 346, 13
- Jones, C. & Forman, W. 1999, ApJ, 511, 65
- Kempner, J. C., Sarazin, C. L., & Ricker, P. M. 2002, ApJ, 579, 236
- Markevitch, M., et al. 2000, ApJ, 541, 542
- Markevitch, M., et al. 2003, ApJ, 586, L19
- Markevitch, M., Gonzalez, A. H., David, L., Vikhlinin, A., Murray, S., Forman, W., Jones, C., Tucker, W., 2002, ApJ, 567, L27
- Markevitch, M., & Vikhlinin, A., 2001, ApJ, 563, 95
- Markevitch, M., Vikhlinin, A., & Mazzotta, P. 2001, ApJ, 562, L153
- Mathis, H., Lavaux, G., Diego, J. M., Silk, J., 2003, MNRAS, submitted (astro-ph/0312015)
- Mazzotta, P., Markevitch, M., Vikhlinin, A., Forman, W. R., David, L. P., & VanSpeybroeck, L. 2001, ApJ, 555, 205
- Mazzotta, P., Fusco-Femiano, R., & Vikhlinin, A. 2002, ApJ, 569, L31
- Nagai, D., & Kravtsov, A., 2003, ApJ, 587, 514
- Plucinsky, P., et al. 2003, SPIE, 4851, 89
- Ricker, P. M., & Sarazin, C. L. 2001, ApJ, 561, 621
- Schindler, S., Müller, E., 1993, A & A, 272, 137
- Ulmer, M. P., Wirth, G. D., Kowalski, M. P., 1992, ApJ, 397, 430
- Vikhlinin, A., Markevitch, M., & Murray, S. S., 2001a, ApJ, 549, L47
- Vikhlinin, A., Markevitch, M., & Murray, S. S., 2001b, ApJ, 551, 160
- Vikhlinin, A. A. & Markevitch, M. L. 2002, Astronomy Letters, 28, 495
- Yang, Y., Zhou, X., Yuan, Q., Jiang, Z., Ma, J., Wu, H., Chen, J., 2004, ApJ, 600, 141